Available online at www.sciencedirect.com
SCIENCE DIRECT®
ELSEVIER
Journal of Magnetism and Magnetic Materials 293 (2005) 8–14
Journal of magnetism and magnetic materials
www.elsevier.com/locate/jmmm

Physical and chemical properties of nanoscale magnetite-based solvent extractant

Ritu D. Ambashta[a], Seikh Mohammad Yusuf[b], Mayuresh D. Mukadam[b], Sher Singh[b], Piaray Kishan Wattal[a], Dhirendra Bahadur[c,*]

[a]*Back-End Technology Development Division, Bhabha Atomic Research Centre, Trombay, India*
[b]*Solid State Physics Division, Bhabha Atomic Research Centre, Trombay, India*
[c]*Department of Metallurgical Engineering & Materials Science, Indian Institute of Technology, Powai, India*

Available online 2 March 2005

Abstract

Nanoscale magnetite bearing magnetic carrier with an adsorbed layer of dibenzo-18-crown-6 was evaluated for removing radionuclides from nuclear waste solutions using magnetically assisted separation method. TEM results indicate that the average size of the base magnetite particles is ~19 nm. The results of Mössbauer spectroscopy and field cooled (FC) and zero field cooled (ZFC) magnetization confirm the superparamagnetic behaviour of the magnetite particles in the polymer beads at room temperature and hence meet the requirement of magnetic filter regeneration capability.

PACS: 75.70

Keywords: Superparamagnetic; Polymer; Magnetite; Nanoparticles; Mössbauer spectroscopy; Extractant; Strontium; Potassium; Magnetic separation; Crown ether; Synthesis

1. Introduction

The extractants, such as, crown ethers in solvated organic medium, find extensive applications for the removal of radionuclides from liquid wastes [1]. Loading the extractants on resins allow lower volume requirements of the extractants for application in column-based separation method [2]. Rendering the resins magnetic enables a less complex and efficient magnetic separation methodology compared to column-based bead extraction [3]. High-gradient magnetic filtration (HGMF) techniques have been widely employed for environmental remediation by magnetic coating and magnetic seeding, respectively. Particles with a diameter larger than superparamagnetic limit

*Corresponding author. Tel.: +91 22 25767632; fax: +91 22 25763480.
E-mail address: dhiren@met.iitb.ac.in (D. Bahadur).

0304-8853/$ - see front matter © 2005 Elsevier B.V. All rights reserved.
doi:10.1016/j.jmmm.2005.01.036

exhibit an undesirable 'magnetic memory' after being exposed to an applied magnetic field. This hinders the magnetic filter regeneration procedure. For HGMF applications, it is therefore, desirable to have superparamagnetic behaviour at room temperature. Single domain particles, whose thermal energy is greater than or equal to the magnitude of magnetic anisotropy energy barrier, exhibit superparamagnetic relaxation [4]. Superparamagnetic magnetite (Fe_3O_4) particles enable efficient filter regeneration capability. The support matrix within which nanostructures are synthesized determine their physical properties in addition to providing a means of particle dispersion [5].

Synthesis of hydrophobically coated magnetite has been reported extensively by generation of magnetite in an emulsion of water–oil [6–8]. In order to allow reactivity of magnetic beads in aqueous media, Sucholeki [9] dispersed hydrophobic particles in aqueous dispersible polymers such as polyvinyl alcohol. Sorption of solvent extractant allows impregnation of extractant on to resin beads [10]. It is reported in the literature that substituted 18-crown-6 forms suitable extractant for the removal of radioactive strontium from nuclear wastes [11].

Here, we present the characterization of crown ether loaded superparamagnetic magnetite-based polymer beads, which find application in magnetically assisted chemical separation of potassium and strontium from aqueous medium.

2. Experimental

2.1. Synthesis

Hydrophobically coated magnetite particles were prepared in water toluene dispersion. An aqueous mixture of 78 mL of iron (III) chloride and iron (II) chloride in stoichiometric ratio was added to a mixture of 130 mL toluene, 78 mL tetramethyl ammonium hydroxide (25% in methanol), 0.6 g cetyl trimethyl ammonium bromide and 1 g polyester (derivative of propylene glycol, isophtalic acid and maleic anhydride) in styrene monomer. The dispersion was ultrasonicated to obtain hydrophobically coated magnetic particles. This formed base magnetite particles. To the dispersion was added 19 g polyester in styrene monomer, 20 μL of dimethyl aniline and 0.2 g benzoyl peroxide and ultrasonicated further for 20 min.

Separately, about 600 g of deionized water was weighed into a 2 L, 4-necked round-bottom flask fitted with a condenser, nitrogen inlet and an overhead stirrer and separating funnels to introduce magnetic dispersion. Water in the flask was heated to 90 °C and purged with nitrogen for 30 min. About 6 g of polyvinyl alcohol (MW 22,000) was added to the flask; a nitrogen blanket is maintained above the liquid surface for the duration of the reaction. The continuous fluid phase was stirred for 30 min at 90 °C, allowed to cool under stirring to 65 °C for about 16 h. This polymer magnetite composite was poured into the continuous fluid phase, pre-cooled to room temperature, and stirring was continued. Reaction was allowed to proceed for 24 h at room temperature to obtain polyester polystyrene polyvinyl alcohol blended magnetic beads.

Tetramethyl ammonium hydroxide dissociates to provide alkaline medium for co-precipitation of ferrous and ferric ions. In addition it also stabilizes dispersion of magnetite in aqueous medium. Stabilization occurs because hydroxyl group gets strongly adhered on the surface of magnetite and the non-polar alkyl chain extends into the solvent. Additionally, cetyl trimethyl ammonium bromide plays the role of co-surfactant that prevents aggregation of the particles by steric mechanism. The polymer embeds the magnetite nanoparticles within its network.

Dibenzo-18-crown-6 (10^{-3} M) was dissolved in a mixture of tributyl phosphate and toluene (1:1.8 v/v) to obtain solvent extractant for potassium. A 2 mL mixture of extractant, acetone and methanol (1:2:1 v/v) were added to 1 g magnetic beads and allowed to stand for 24 h. Air-dried samples were used for extraction studies.

2.2. Characterization

Philips Model CM200 TEM, operating at 180 keV, was used for imaging the samples. Electron diffraction (SAED) was carried out on

selected areas of the particles. For the analysis of iron content in the magnetic polymer beads, the sample was first mixed with twice the amount of potassium bisulphate and heated in platinum crucible at 500 °C. The residue was dissolved in hot concentrated nitric acid. The iron estimation was followed by a treatment of solution with ammonium thiocyanate to form iron thiocyanate. Calibration with respect to standard iron solutions was used to estimate the concentration of iron in the present sample by measuring absorbance of iron thiocyanate complex at 565 nm using an UV-visible spectrometer (UV-160A Shimadzu). Dynamic Light Scattering Unit (Malvern Master Sizer 2000) was used to determine the size of magnetic polymer beads. The DC magnetization measurements were carried out using 12 T (Oxford Instruments) vibrating sample magnetometer as a function of magnetic field and temperature. For zero field cooled (ZFC) magnetization measurements, the sample was first cooled from room temperature down to 5 K in zero field. After applying 100 Oe field at 5 K, the magnetization was measured in the warming cycle. Whereas, for field cooled (FC) magnetization measurements, the sample was cooled in the same field (100 Oe) down to 5 K and the magnetization was measured in the warming cycle under the same field. Mössbauer spectra were recorded with a 50 mCi of ^{57}Co in Rh source at 300, 142, 98, 78 and 62 K. Each spectrum was folded with respect to calibration spectrum of α-iron using Recoil Demo (Mössbauer Analysis Software) program and shift velocity parameters were determined.

Flame photometer (Systronics 128) was used for the estimation of potassium. Solution of potassium was aspirated through LPG flame. The emitted light was collected through optical lenses and passed on to photodetector through potassium filter. Calibration with respect to standard potassium solution was used to estimate concentration of potassium.

Sodium iodide (thallium)-based gamma detector was used for counting activity of radiotracer strontium ($^{85+89}$Sr).

Base magnetite particles were characterized by TEM only. Magnetic polymer beads were characterized using UV-visible spectrometry, TEM, VSM, Mössbauer spectrometry and dynamic light scattering. Crown ether loaded magnetic beads were characterized with respect to potassium and strontium extraction capability.

In order to investigate the extraction behaviour of potassium and strontium, 1.5 mL of 100 ppm of potassium (potassium nitrate) and strontium (strontium nitrate) were separately contacted with 30 mg of crown ether loaded magnetic beads. Strontium solution was spiked with $^{85+89}$Sr tracer. The solution after an hour equilibration time was held on magnet and supernatant was assayed for potassium content using flame photometer and strontium content using gamma detector.

3. Results and discussion

Fig. 1 shows the bright field TEM image of the base magnetite particles. The particle size distribution was extracted from this image and represented well by a lognormal distribution function with an average particle size of 19 nm. The selected area electron diffraction pattern (SAED) is shown in Fig. 2. The pattern consists of rings corresponding to FCC planes of magnetite confirming the formation of magnetite [12]. The observed ring pattern indicates a random orientation of the nanocrystalline magnetite particles.

From the UV-visible spectrometry, the Fe_3O_4 content in the magnetic polymer beads was estimated to be 12% by weight. The particle size distribution of the polymer loaded magnetite beads, evaluated by dynamic light scattering method, is shown in Fig. 3. Majority of the beads are having a mean diameter of 10 μm. Fig. 4 shows the TEM image of the polymer loaded magnetite beads indicating a non-uniform agglomeration. The clustered nature of the particles suggests a random precipitation of the magnetic particles within a polymer having random coil structure. Coating (with polymer) of magnetite particles is evident from the observed diffused nature of the diffraction pattern.

Field (H) dependence of DC magnetization (M) at 300 and 5 K is shown in Fig. 5. From M vs. H data, the average size of the magnetic particles was

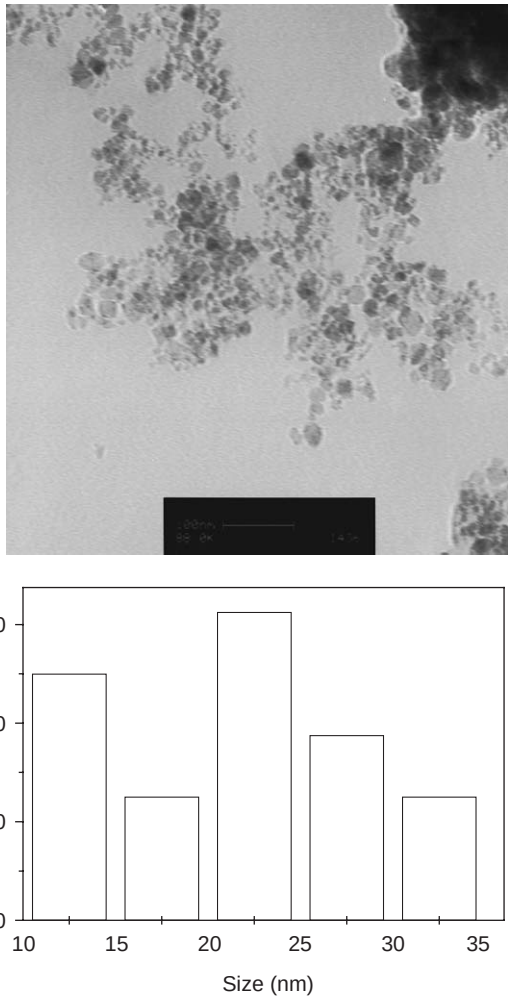

Fig. 1. Top: TEM image (Scale 100 nm) of the base magnetite particles. Bottom: particle size distribution.

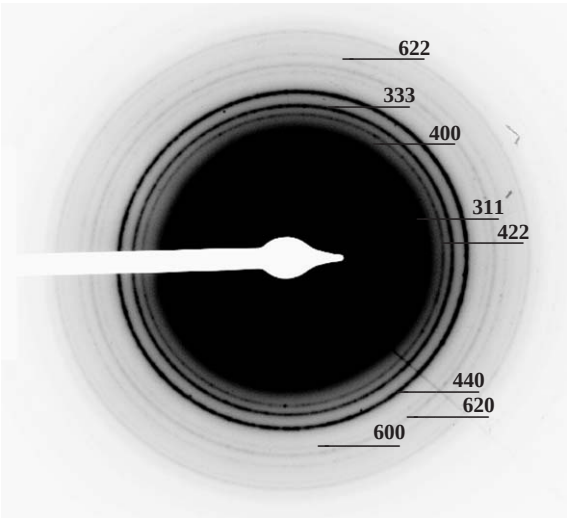

Fig. 2. SAED on the base magnetite particles.

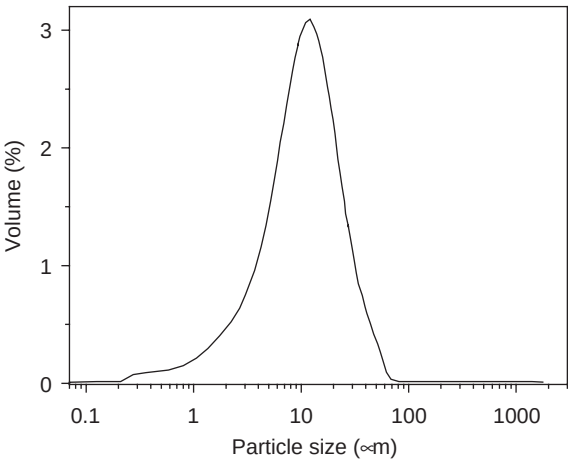

Fig. 3. Particle size distribution obtained from dynamic light scattering experiments.

calculated using the expression [14]

$$D_m = \left(\frac{18kT}{M_s \pi} \left[\frac{\chi_i}{3} \left(\frac{1}{H_0} \right) \right]^{1/2} \right)^{1/3}, \quad (1)$$

where k is the Boltzman constant, T is the temperature, M_S is the saturation magnetization, χ_i is the initial susceptibility, $1/H_0$ is the extrapolation to the abscissa of a plot of M against $1/H$ at high fields, and D_m is the volume fraction median diameter. The above equation is valid only for non-interacting magnetic particles, such as, well-dispersed ferrofluids [13–15]. For dry powders, the low field magnetization may differ from the Langevin behaviour due to interparticle interactions. However, in the present sample, as indicated by diffused ring pattern, the polymer either encapsulates the ferrofluid-type liquid within its structure or magnetite particles in small clusters are coated completely by the polymer and hence expected to be non-interacting as in diluted ferrofluids. Therefore, the above equation can be

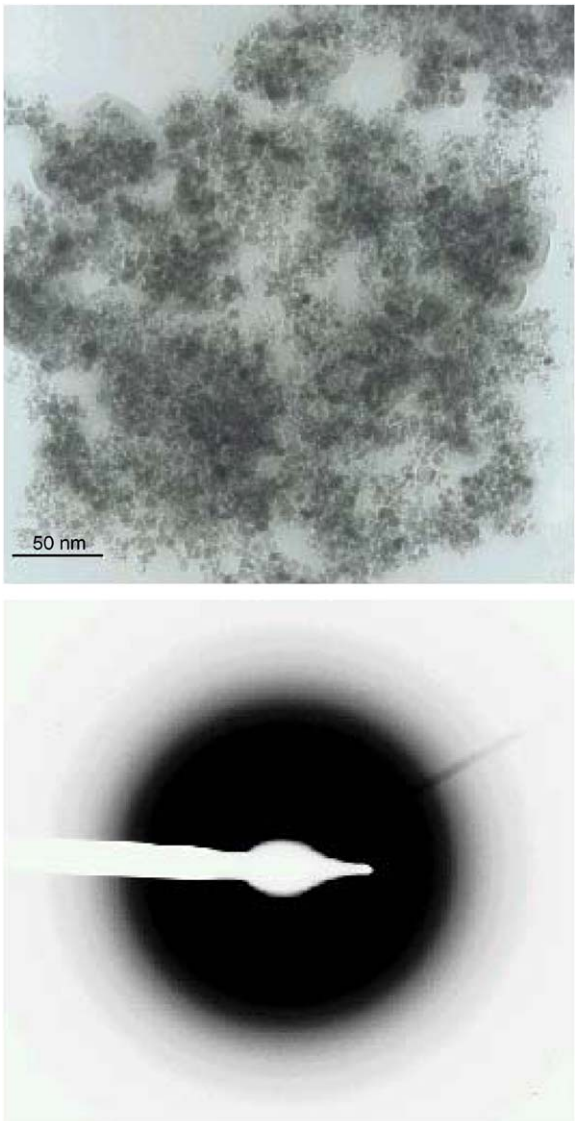

Fig. 4. Top: TEM image (scale 50 nm). Bottom: SAED of the magnetic polymer beads.

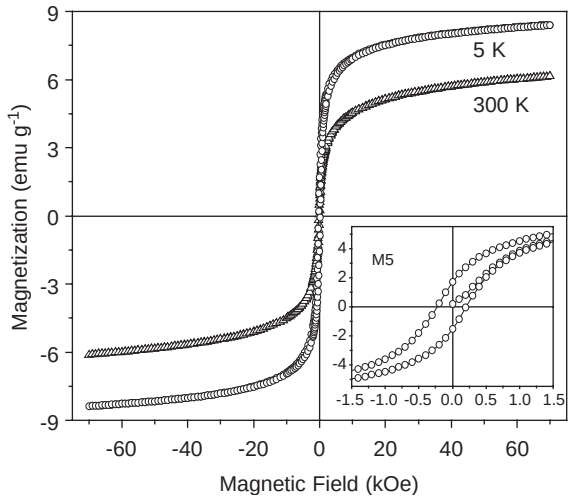

Fig. 5. Hysteresis loops recorded at 300 and 5 K. Inset shows the low field region of the hysteresis loop at 5 K.

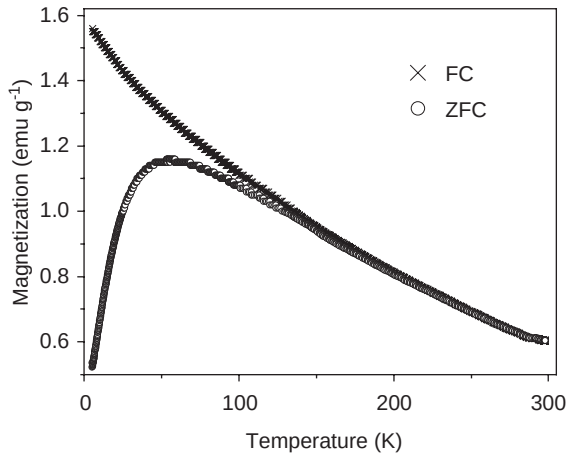

Fig. 6. Field cooled and zero field cooled magnetization curves for the magnetic polymer beads at 100 Oe.

used for deriving the average magnetic particle size. The average diameter of the magnetic particles using the Eq. (1) is evaluated to be about 16 nm.

Fig. 6 depicts the temperature dependence of ZFC and FC magnetization under the applied field of 100 Oe.Thermomagnetic irreversibility is observed below about 120 K. A broad peak in the ZFC magnetization is found at about 56 K. Such type of behaviour is usually observed in superparamagnetic systems consisting of single domain particles. At sufficiently low temperatures, the moment of these particles freeze/block in random orientations as dictated by the magnetocrystalline anisotropy. The temperature below which these particles are blocked is called blocking temperature. Above blocking temperature, these particles

respond to an external magnetic field like paramagnetic atoms/ions. However, the individual particle moment is large compared to that of paramagnetic atoms/ions. If there is a distribution in the particle size and hence anisotropy energy, the blocking and unblocking processes occur over wide temperature range giving broad peak in ZFC magnetization curve. Such kind of broad peak in ZFC magnetization and branching in ZFC and FC magnetization were observed by López Pérez et al. [16] in their studies on magnetite with different mean sizes.

The Mössbauer spectra recorded at 300, 142, 98, 78 and 62 K are shown in Fig. 7. At 300 K, the observed nearly collapsing nature of the magnetic hyperfine splitting indicates the majority of the magnetite particles are unblocked and having superparamagnetic relaxation. At a given temperature, the area ratio of superparamagnetic and ferrimagnetic components reflects the relative number of particles that are above and below the blocking temperature [17–19]. The temperature dependence of the area ratio is plotted in Fig. 8. It indicates that at about 115 K, 50% of the particles are blocked.

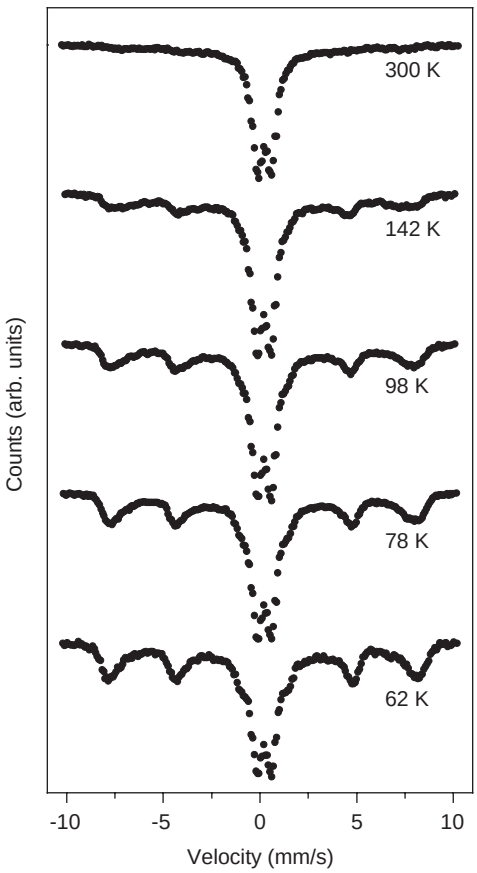

Fig. 7. Mössbauer spectra of the magnetic polymer beads recorded at various temperatures.

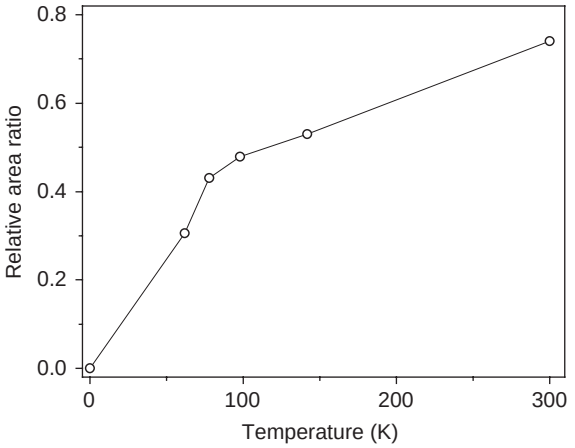

Fig. 8. Superparamagnetic to ferrimagnetic component relative area vs. temperature.

In order to examine the surface extraction behaviour of the crown ether loaded magnetic polymer beads, magnetically assisted chemical separation was studied for the removal of potassium and strontium from aqueous medium. Distribution coefficient, K_d, relates to the extraction capacity of the sorbents. It is expressed using the relation

$$K_d = \left(\frac{C_i - C_f}{C_f}\right)\frac{V}{m}, \tag{2}$$

where C_i and C_f are initial and final concentrations of elements in solution before and after extraction, V is the volume of solution and m is the mass of solvent loaded magnetic beads. Fig. 9 shows a comparison in the extraction behaviour of potassium and strontium by the magnetite-based solvent extractant. The crown ether is capable of forming stable complex with potassium ion. The stability of the complex is on account of ionic radius cavity size compatibility. Solvent impregnation may be by pore filling and surface adsorp-

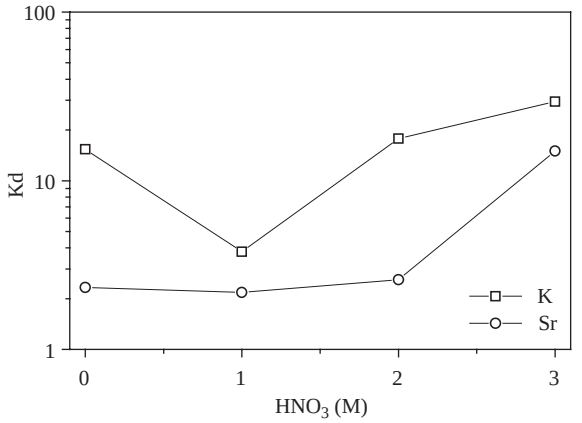

Fig. 9. Distribution coefficient for strontium with respect to nitric acid concentration.

tion mechanism. Tributyl phosphate and crown ether as well as the polymer resin have polar groups. The polar interactions may have enabled the cohesion of solvent on surface of the magnetic beads. On contacting with aqueous solution of potassium ions, the cation is drawn strongly to the cavity of extractant leading to its capture on the magnetic bead. Strontium ion being smaller than potassium shows slightly lowered uptake.

4. Conclusion

Randomly precipitated nanoparticles of magnetite within polyester polystyrene structure were characterized. The blocking temperature obtained from Mössbauer and magnetization studies indicates that the majority of particles are superparamagnetic at room temperature and therefore, possess filter regeneration capability. The impregnation of extractant enables potassium and strontium extraction capability. The extractant loaded magnetic beads possess bulk superparamagnetic property and surface decontamination behaviour. The beads with suitable extractants may form potential systems for radionuclide removal from aqueous wastes.

Acknowledgements

The authors thank Dr. Ramanathan from MSD-BARC for dynamic light scattering data and DB acknowledges Dept. of Science and Technology, Govt. of India for financial support.

References

[1] M.K. Bekemisev, C.M. Wai, Separation Technology in Nuclear Waste Management, CRC Press, Boca Raton, FL, 1996, p. 47.
[2] R. Juang, Proc. Natl. Sci. Counc. ROC (A) 23 (1999) 353.
[3] L. Nunez, M.D. Kaminski, J. Magn. Magn. Mater. 194 (1994) 102.
[4] G.P. Hatch, R.E. Stelter, J. Magn. Magn. Mater. 225 (2001) 262.
[5] P.A. Dresco, V.S. Zaitsev, R.J. Gambino, B. Chu, Langmuir 15 (1999) 1945.
[6] K.M. Lee, C.M. Sorenson, K.J. Klabnde, G.C. Hadjipanayos, IEEE Trans. Magn. 28 (1992) 3180.
[7] K. Liz, M.A. López Quintela, J. Mira, J. Rivas, J. Mater. Sci. 29 (1994) 3797.
[8] I. Safarik, M. Safarikova, Monatsh. Chem. 133 (2002) 737.
[9] I. Sucholeiki, US Patent No. 5858534, January 12, 1999.
[10] M.L. Dietz, E.P. Horwitz, D.M. Nelson, M. Wahlgron, Health Phys. 61 (1991) 871.
[11] W.W. Schulz, L.A. Bray, Sep. Sci. Technol. 22 (1987) 191.
[12] Y. Hou, J. Yu, S. Gao, J. Mater. Chem. 13 (2003) 1983.
[13] R.W. Chantrell, J. Popplewell, S.W. Charles, IEEE Trans. Magn. 16 (1980) 975.
[14] M. Blanco-Mantecón, K. O'Grady, J. Magn. Magn. Mater. 203 (1999) 50.
[15] J. Popplewell, L. Sakhnini, J. Magn. Magn. Mater. 149 (1995) 72.
[16] J.A. López Pérez, M.A. López Quintella, J. Mira, et al., J. Phys. Chem. B 101 (1997) 8045.
[17] S. Mørup, H. Topsoe, J. Appl. Phys. 11 (1976) 63.
[18] S. Mørup, J.A. Dumesic, H. Topsoe, Applications of Mössbauer Spectroscopy II, Academic Press, New York, 1980, p. 23.
[19] A.F. Lehlooh, S.H. Mahmood, J. Magn. Magn. Mater. 151 (1995) 163.